Some Features of the Physical Properties of Rare-Earth Iron Garnets Near the Compensation Temperature

A. K. ZVEZDIN AND V. M. MATVEEV

Submitted April 26, 1971

Zh. Eksp. Teor. Fiz. **62**, 260–271 (January, 1972)

Phase diagrams of ferromagnetic substances with two sublattices in a magnetic field are investigated. Cases of uniaxial and cubic anisotropy are considered. The types of phase transitions between various phases in the ferromagnetic substances are determined. They are transitions of the "orientation" type, i.e., the ordering parameters in them are the angles between the magnetic sublattices and the crystallographic axes. It is noteworthy that in relatively weak magnetic fields ($H \ll 10^6$ Oe) the transitions are very sharp and can be described satisfactorily by the Landau theory. The behavior of the Faraday effect on variation of temperature and magnetic field strength is considered.

INTRODUCTION

MANY rare-earth ion garnets (RIG) have a compensation point at which the sign of the complete magnetization M_S of the crystal is reversed. Near the compensation temperature, the RIG exhibit many anomalies of different physical quantities—the coercive force, Young's modulus, the specific rotation of the plane of polarization of the light, the magnetocaloric effect, etc.

It is well known[1] that in ferrimagnets with two sublattices, in a certain interval of magnetic fields $H_1^{cr} < H < H_2^{cr}$, a flipping of the sublattices from an antiparallel arrangement to a parallel one takes place. Such a situation arises in RIG[2,3], for which the two-sublattice model is well applicable (at $H \ll 10^6$ Oe). In the isotropic case, the critical fields H_1^{cr} and H_2^{cr} are given approximately by the expressions

$$H_1^{cr} = \frac{M_1 - M_2}{(M_{10}M_{20})^{1/2}} H_0, \quad H_2^{cr} = \frac{M_1 + M_2}{(M_{10}M_{20})^{1/2}} H_0, \tag{1.1}$$

where M_1 and M_2 are the sublattice magnetizations at a given temperature, $M_{10} = M_1(T = 0°K)$, $M_{20} = M_2(T = 0°K)$, and H_0 is proportional to the exchange field acting between the sublattices.

In garnets, $H_1^{cr} \approx 5 \times 10^5$ Oe at $T = 0°K$, but, as can be seen from (1.1), the flipping near the compensation temperature T_c takes place in arbitrarily weak fields ($H_1^{cr} \to 0$). On the one hand, this indicates that the singularities of the physical quantities are apparently connected just with the flipping of the sublattices. On the other hand, the behavior of the RIG near T_c will be strongly influenced by the magnetocrystallographic anisotropy[4], which was not taken into account in[1-3].

In the present paper we attempt to construct a thermodynamic theory of the physical phenomena in RIG near T_c, with allowance for the flipping of the sublattices and the anisotropy in a large interval of external magnetic fields. The equilibrium states and critical fields in a three-sublattice anisotropic ferrimagnet at $T = 0°K$ were obtained in[5].

2. MAGNETIC STRUCTURE AND THERMODYNAMIC POTENTIAL OF RIG

RIG are three-sublattice ferrimagnets. Their magnetic structure is determined by the strong antiferromagnetic interaction between the Fe^{3+} ions at the crystallographic sites d and a ($H_1^{exch} = 1.7 \times 10^6$ Oe), which leads to an antiparallel binding of the sublattices {d} and {a}, and a much weaker antiferromagnetic interaction between the resultant iron and rare-earth sublattices ($H_2^{exch} = 3 \times 10^5$ Oe). We note that the RIG model in which {a} and {d} sublattices are combined into a single {a − d} sublattice is applicable in external fields $H < H_1^{exch}$. The very weak interaction between the rare-earth ions ($H_3^{exch} = 10^3$ Oe) can be disregarded already at $T \gtrsim 10°K$. The {R} sublattice constitutes in essence a system of paramagnetic ions situated in the exchange field $\mathbf{H}_2^{exch}$. The field $\mathbf{H}_2^{exch}$ acts only on the spin. If the rare-earth ion has a total mechanical angular momentum J different from the spin, then the magnetization of the {R} sublattice in an external field **H** will be determined by the effective field[6]

$$\mathbf{H}_{eff} = \frac{2(g_J - 1)}{g_J} \mathbf{H}_2^{exch} + \mathbf{H}, \tag{2.1}$$

where g_J is the Lande factor.

The concrete dependence of the magnetization of the rare-earth sublattice on the effective field and on the temperature is determined by the spectrum of the rare-earth ion in the crystal field, and the explicit form of the function $M_R = M_R(T, H_{eff})$ influences only the quantitative results and is of no importance for the obtaining of qualitative conclusions. We assume this dependence in the form

$$M_R = M_{R0} B_S(\mu_R H_{eff} / kT), \tag{2.2}$$

where $B_S(x)$ is the Brillouin function ($M_{R_0} = M_R(T = 0°K)$, μ_R is the magnetic moment of the rare-earth ion, H_{eff} is given by (2.1), and k is the Boltzmann constant. In GdIG in the ground state, the orbital angular momentum is L = 0, and therefore (2.2) describes correctly the course of the magnetization of the gadolinium sublattice. In YbIG, owing to the strong influence of the crystalline field, the ground state is a doublet separated by a large energy gap (500 cm^{-1}) from the excited levels[7]. Thus, formula (2.2) is also sufficiently accurate for YbIG in a wide temperature interval (at S = 1/2).

Recognizing that $\mathbf{H}_2^{exch} = \lambda_{Fe-R}\mathbf{M}_{Fe}$ (λ_{Fe-R} is the exchange constant), we obtain from (2.1)

$$H_{eff} = \left| \mathbf{H} + \frac{2(g_J - 1)}{g_J} \lambda_{Fe-R} \mathbf{M}_{Fe} \right| = (H^2 + \lambda^2 M_{Fe}^2 - 2\lambda M_{Fe} H \cos\theta)^{1/2}. \tag{2.3}$$

We have put here $\lambda = 2(g_J - 1)|\lambda_{Fe-R}|/g_J$, where θ is the angle between the vectors **H** and $\mathbf{M}_{Fe}$.

The anisotropy in RIG is apparently of the single-ion type[8], i.e., the iron and rare-earth sublattices make independent contributions to the total anisotropy energy $W_a = W_{Fe} + W_R$:

$$W_a = K_{Fe} f(\theta_{Fe}, \varphi_{Fe}) + K_R f(\theta_R, \varphi_R). \quad (2.4)$$

Here K_{Fe} and K_R are respectively the anisotropy constants of the iron and of the rare-earth sublattices, the angles θ_{Fe}, φ_{Fe}, and θ_R, φ_R define the directions of the magnetic moments $\mathbf{M}_{Fe}$ and $\mathbf{M}_R$, while the explicit form of the function $f(\theta, \varphi)$ is specified by the symmetry of the crystal. RIG are cubic ferrimagnets. We shall also consider the case of uniaxial anisotropy. Namely, uniaxial "induced" anisotropy is frequently realized in magnetooptical experiments with thin garnet plates[9]. In addition, mixed iron garnets with uniaxial anisotropy have recently been synthesized[10], and the theory developed below can be applied to them.

The anisotropy energy of all RIG near T_c is much smaller than the exchange energy, and it can therefore be assumed that $\mathbf{M}_R \parallel \mathbf{H}_{eff}$, i.e., the angles θ_R and φ_R can be replaced by the angles θ' and φ', which define the orientation of the vector $\mathbf{H}_{eff}$ relative to the crystallographic axes.[1)] Taking into account the weak dependence of the iron-sublattice magnetization on the temperature and on the magnetic field near T_c, we write the thermodynamic potential of the RIG in the form[2)]

$$\Phi = -MH\cos\theta - \int_0^{H_{eff}} M_R\, dH_{eff} + K_{Fe} f(\theta_{Fe}, \varphi_{Fe}) + K_R f(\theta', \varphi'), \quad (2.5)$$

where H_{eff} and θ are taken from (2.3) and $M = M_{Fe}(T_c)$. As shown in the Appendix, in fields $H \ll \lambda M$ we can use the simpler expression

$$\Phi = -MH\cos\theta - \int_0^{H_{eff}} M_R\, dH_{eff} + Kf(\theta_{Fe}, \varphi_{Fe}), \quad (2.6)$$

where $K > 0$ is the experimentally-measured anisotropy constant of the crystal. We note the case of GdIG, in which the anisotropy energy is determined practically completely by the iron sublattice.

Let **i**, **j**, and **k** be the unit vectors of a rectangular coordinate system, and θ and φ the polar angles of the vector **M** relative to this system. Then, for a uniaxial crystal and at **H** parallel to the easy axis (EA) we have $f(\theta, \varphi) \equiv f(\theta) = -\cos^2\theta$ in the coordinate system $\{\mathbf{i}, \mathbf{j}, \mathbf{k}\} = \{\mathbf{i} \perp \mathbf{n}, [\mathbf{ni}], \mathbf{n}\}$, where **n** is a unit vector in the EA direction. If $\mathbf{H} \perp$ EO, then the function $f(\theta, \varphi)$ takes in the coordinate system $\{\mathbf{i}, \mathbf{j}, \mathbf{k}\} = \{\mathbf{n}, \mathbf{H} \times \mathbf{n}/H, \mathbf{H}/H\}$ the form $f(\theta, \varphi) = -\sin^2\theta\cos^2\varphi$. For a cubic RIG at $\mathbf{H} \parallel [111]$ in the coordinate system $\{\mathbf{i}, \mathbf{j}, \mathbf{k}\} = \{[1\bar{1}0], [11\bar{2}], [111]\}$ we have

$$f(\theta, \varphi) = {}^1/_3\sqrt{2}\cos\theta\sin^3\theta\sin 3\varphi - {}^1/_3\cos^4\theta - {}^1/_4\sin^4\theta, \quad (2.7)$$

and finally, when $\mathbf{H} \parallel [100]$ and $\{\mathbf{i}, \mathbf{j}, \mathbf{k}\} = \{[100], [010], [001]\}$ we have

$$f(\theta, \varphi) = -{}^1/_4(\sin^2 2\theta + \sin^4\theta\sin^2 2\varphi). \quad (2.8)$$

We assume that in the cubic case the easy-magnetization direction is [111].

The conditions under which the thermodynamic potential (2.6) has extremal values with respect to the angles θ and φ are

$$\frac{\partial\Phi}{\partial\theta} = MH\sin\theta - M_R\frac{dH_{eff}}{d\theta} + K\frac{\partial f}{\partial\theta} = 0,$$
$$\frac{\partial\Phi}{\partial\varphi} = K\frac{\partial f}{\partial\varphi} = 0 \quad (2.9)$$

and can be written with the aid of (2.3) in the form

$$\partial\Phi/\partial\theta = MH(1 - \lambda\chi_\theta)\sin\theta + K\,\partial f/\partial\theta = 0,$$
$$\partial\Phi/\partial\varphi = K\,\partial f/\partial\varphi = 0, \quad (2.10)$$

where $\chi_\theta = \chi(\theta, H, T) = M_R/H_{eff}$. Equations (2.10) have in all the considered cases the solutions $\{\theta = 0\}$ and $\{\theta = \pi\}$. These solutions correspond to the minimum of Φ if $\partial^2\Phi/\partial\theta^2|_{\theta=0} > 0$ and $\partial^2\Phi/\partial\theta^2|_{\theta=\pi} > 0$, respectively. The boundaries of the stability region of the collinear phases $\{\theta = 0\}$ and $\{\theta = \pi\}$ (these are the lines AA′ and BB′ in Figs. 1–4) are determined by the equations $\partial^2\Phi/\partial\theta^2|_{\theta=0} = 0$, and $\partial^2\Phi/\partial\theta^2|_{\theta=\pi} = 0$. For example, in the uniaxial case

$$MH(1 - \lambda\chi_0) \pm 2K = 0, \quad MH(1 - \lambda\chi_\pi) \mp 2K = 0. \quad (2.11)$$

The upper sign corresponds to $\mathbf{H} \parallel$ EA and the lower sign to $\mathbf{H} \perp$ EO. For a cubic crystal at $\mathbf{H} \parallel [100]$ it is necessary to take the lower signs in (2.11), and at $\mathbf{H} \parallel [111]$ it is necessary to take the upper signs and replace 2K by 4K/3.

In addition, in a certain interval of magnetic fields and temperatures, there are solutions with $\theta \neq 0$ and π (angle phases). The values $\theta = \theta_0$ and $\varphi = \varphi_0$ are determined at specified H and T from the system of equations

$\mathbf{H} \parallel$ EA $\quad MH(1 - \lambda\chi_\theta) + 2K\cos\theta = 0;$ (2.12a)

$\mathbf{H} \perp$ EA $\quad \begin{cases} MH(1 - \lambda\chi_\theta) - 2K\cos\theta\cos^2\varphi = 0, \\ 2K\sin^2\theta\cos\varphi\sin\varphi = 0; \end{cases}$ (2.12b)

$\mathbf{H} \parallel [111]$ $\quad \begin{cases} MH(1 - \lambda\chi_\theta) + K({}^4/_3\cos^3\theta - \sin^2\theta\cos\theta - \\ - {}^1/_3\sqrt{2}\sin^3\theta\sin 3\varphi + \sqrt{2}\cos^2\theta\sin\theta\sin 3\varphi) = 0, \\ \sqrt{2}K\cos\theta\sin^3\theta\cos 3\varphi = 0; \end{cases}$ (2.12c)

$\mathbf{H} \parallel [100]$ $\quad \begin{cases} MH(1 - \lambda\chi_\theta) - K\cos\theta(2\cos 2\theta + \sin^2\theta\sin^2 2\varphi) = 0, \\ -K\sin^4\theta\sin 2\varphi\cos 2\varphi = 0. \end{cases}$ (2.12d)

It is easy to verify that at the extremal points we have $\partial^2\Phi/\partial\theta\partial\varphi|_{\theta_0, \varphi_0} = 0$, and therefore the solution $\{\theta_0, \varphi_0\}$ will correspond to a minimum if $\partial^2\Phi/\partial\varphi^2 > 0$ and $\partial^2\Phi/\partial\theta^2 > 0$. From this we obtain with the aid of (2.12) the following equilibrium values of the angle φ: φ_0 is arbitrary at $\mathbf{H} \parallel$ EA, $\varphi_0 = 0, \pi$ at $\mathbf{H} \perp$ EA, $\varphi_0 = \pi/4, 3\pi/4, 5\pi/4, 7\pi/4$ at $\mathbf{H} \parallel [100]$, $\varphi_0 = \pi/2, 7\pi/6, 11\pi/6$ for $0 < \theta < \pi/2$ and $\varphi_0 = \pi/6, 5\pi/6, 3\pi/2$ for $\pi/2 < \theta < \pi$ at $\mathbf{H} \parallel [111]$.

Thus, if the magnetic field is directed along the EA of the crystal, then there is a nondenumerable number of solutions $\{\theta_0, \varphi\}$ which differ in the angle φ, all of which correspond to the same energy ("degeneracy"). At $\mathbf{H} \parallel$ EA there are two solutions with one energy, $\{\theta_0, 0\}$ and $\{\theta_0, \pi\}$. In the cubic case the angle solutions have fourfold ($\mathbf{H} \parallel [100]$) or threefold ($\mathbf{H} \parallel [111]$) degeneracy.

[1)] We regard the rare-earth sublattice as a gas of paramagnetic ions, and it is therefore natural for the paramagnetic system to have at $W_R \ll \lambda M^2$ one stable state with a magnetization along the vector $\mathbf{H}_{eff}$.

[2)] S. V. Tyablikov[1] has investigated in his monograph the flipping of the sublattices in ferrimagnets on the basis of the microscopic model (without allowance for the anisotropy). It can be shown that the thermodynamic potential obtained in[1] reduces under our conditions to expression (2.5) (at $W_a = 0$).

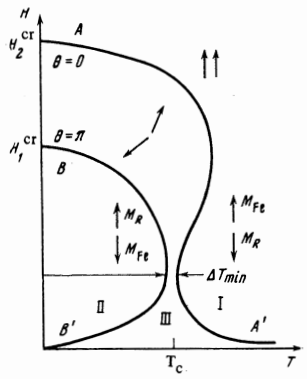

FIG. 1

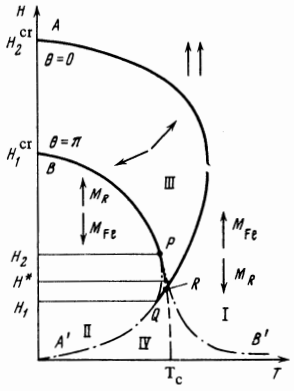

FIG. 2

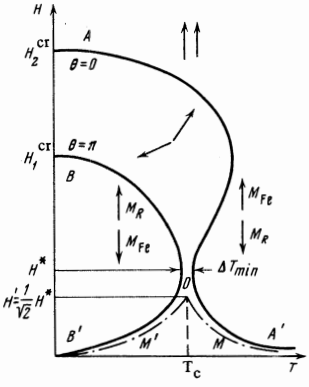

FIG. 3

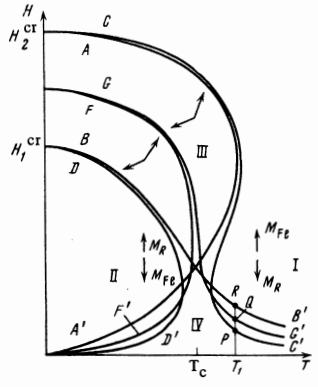

FIG. 4

FIG. 1. Phase diagram of uniaxial ferrimagnet. The magnetic field **H** is perpendicular to the EA of the crystal.

FIG. 2. Phase diagram of uniaxial ferrimagnet at **H** ∥ EA. P is the critical point at which the second-order phase-transition line BP goes over into the first-order phase-transition line PRT_c. PA′ and PB′ are the limits of the stability region of the metastable phases.

FIG. 3. Phase diagram of cubic RIG at **H** ∥ [100]. AA′ and BB′ are the second-order phase-transition lines, OT_c is the first-order phase-transition line, OM and OM′ are the limits of stability of the metastable phases, and O is the critical point.

FIG. 4. Phase diagram of RIG at **H** ∥ [111]. AA′ and BB′ are the phase stability-loss lines $\{\theta = 0\}$ and $\{\theta = \pi\}$, respectively, CC′ and FF′ are the limits of the stability region of the states $\{0 < \theta < \pi/2; \varphi = \pi/2, 7\pi/6, 11\pi/6\}$, and DD′ and GG′ are the limits of the stability region of the states $\{\pi/2 < \theta < \pi; \varphi = \pi/6, 5\pi/6, 3\pi/2\}$.

3. (H, T) PHASE DIAGRAMS OF RIG

The simplest phase diagram is possessed by a uniaxial crystal at **H** ⊥ EA (Fig. 1). The stable phase is $\{\theta = 0\}$ in region I and $\{\theta = \pi\}$ in region II. In region III, the minimum of the potential is realized at values of the angle θ different from 0 and π—flipping of the sublattices takes place. The angle changes from $\theta = 0$ on the line AA′ to $\theta = \pi$ on the line BB′. The expansion of Φ in powers of θ near AA′ takes the form

$$\Phi(H, T, \theta) = \Phi_0(H, T) + a(H, T)\theta^2 + b(H, T)\theta^4 + \ldots, \quad (3.1)$$

with a(H, T) = 0 and b(H, T) > 0 on the line AA′ itself. Therefore the transition from the collinear phase $\{\theta = 0\}$ to the angle phase is a second-order phase transition in accordance with Landau's theory of phase transitions[11]. The ordering parameter in this case is the angle θ. All the foregoing is also valid for the transition from the collinear phase $\{\theta = \pi\}$ into the angle phase. The expansion of the thermodynamic potential in powers of $\pi - \theta$ near the line BB′ takes the form

$$\Phi(H, T, \theta) = \Phi'(H, T) + a'(H, T)(\pi - \theta)^2 + b'(H, T)(\pi - \theta)^4 + \ldots, \quad (3.2)$$

where a′(H, T) = 0 and b′(H, T) > 0 on BB′.

If **H** is parallel to the easy axis of the crystal, then the phase diagram (Fig. 2) contains a region IV, where both collinear phases are stable. RT_c is the first-order phase-transition line on which $\Phi(\theta = 0) = \Phi(\theta = \pi)$.

If, as in the case **H** ⊥ EA, we write out the expansions (3.1) and (3.2), then the lines AA′ and BB′ will have points where the coefficients b(H, T) or b′(H, T) vanish (the points Q and P). Above these points on lines AA′ and BB′, the transition to the angle phase is a second-order transition (b > 0). At the point P, the coefficient of the term $(\pi - \theta)^6$ in the expansion (3.2) is positive. In Landau's theory of phase transitions, such a point is the critical point of the transition of the second-order phase-transition line into the first-order phase transition line[11]. The latter (PR on Fig. 2) can be obtained by eliminating θ_0 from the system:

$$\Phi(\theta_0) = \Phi(\pi), \quad \partial\Phi/\partial\theta|_{\theta=\theta_0} = 0. \quad (3.3)$$

On the curve PQ, the angle phase loses stability and the system goes over jumpwise into the phase $\{\theta = \pi\}$. The jump of the angle θ increases from $\Delta\theta = 0$ at the point P to $\Delta\theta = \pi$ at the point Q. The temperature dependence of the field on the line PQ is obtained from the system of equations (by eliminating θ_0)

$$\partial\Phi/\partial\theta|_{\theta=\theta_0} = 0, \quad \partial^2\Phi/\partial\theta^2|_{\theta=\theta_0} = 0. \quad (3.4)$$

The diagram shows the results of a numerical solution of the equations (for GdIG).

At **H** ∥ [111] of a cubic ferrimagnet, the flipping of the sublattices is from one of the planes (110) ($\varphi = \pi/4, 5\pi/4$) or ($1\bar{1}0$) ($\varphi = 3\pi/4, 7\pi/4$), but in contrast to the phase diagram of Fig. 1, the flipping is not continuous. The phase diagram (Fig. 3) has a region bounded by the curves OM and OM′ where two solutions differing in the angle θ are stable, namely $\{\theta = \theta_1, \varphi_0\}$, and $\{\theta = \theta_2, \varphi_0\}$. The values of θ_1 and θ_2 can be obtained from the first equation in (2.12c) by putting in it $\varphi_0 = \pi/4, 3\pi/4, 5\pi/4, 7\pi/4$. The limits of the metastability region OM′ and OM are determined from the system

$$(\sin\theta)^{-1}\partial\Phi/\partial\theta = MH(1 - \lambda\chi_\theta) - K\cos\theta(3\cos^2\theta - 1) = 0,$$
$$\partial^2\Phi/\partial\theta^2 = -MH\lambda\partial\chi_\theta/\partial\theta + K\sin\theta(9\cos^2\theta - 1) = 0. \quad (3.5)$$

The angle θ changes jumpwise on OM when the temperature is increased, and on OM′ when it is decreased, i.e., there is a temperature hysteresis of the angle (Fig. 5). The jump is $\Delta\theta = 0$ at the point O and increases to $\Delta\theta = 2\cos^{-1}\sqrt{2/3}$ in weak fields. It is interesting that O is the critical point, as for example in a vapor-liquid phase transition. The analog of the density in our case is the flipping angle.

When the external magnetic field is oriented along the easy axis [111] of a cubic ferrimagnet, the limits AA′ and BB′ of the stability regions of the collinear phases are no longer simultaneously second-order phase-transition lines. Even in strong fields, the flipping angle θ changes jumpwise on them. This is connected with the fact that the expansion (2.6) of the thermo-

dynamic potential with $f(\theta, \varphi)$ from (2.7) contains a cubic term. Jumps of the angle occur also on the curves CC′, DD′, FF′, and GG′. The curves FF′ and CC′ are the limits of the stability region of the angle phases $\{0 < \theta_0 < \pi/2,\ \varphi_0 = \pi/2,\ 7\pi/6,\ 11\pi/6\}$. They are determined from the following equations:

$$MH(1-\lambda\chi_{\pi/2}) + {}^1/_3\sqrt{2}K = 0 \text{ for } FF', \qquad \partial\Phi/\partial\theta|_{\theta=\theta_0} = 0,\ \partial^2\Phi/\partial\theta^2|_{\theta=\theta_0} = 0 \text{ for } CC'. \tag{3.6}$$

Analogous equations specify the boundaries GG′ and DD′ of the stability region of the phases $\{\pi/2 < \theta_0 < \pi,\ \varphi_0 = \pi/6,\ 5\pi/6,\ 3\pi/2\}$:

$$MH(1-\lambda\chi_{\pi/2}) - {}^1/_3\sqrt{2}K = 0 \text{ for } GG', \qquad \partial\Phi/\partial\theta|_{\theta=\theta_0} = 0,\ \partial^2\Phi/\partial\theta^2|_{\theta=\theta_0} = 0 \text{ for } DD'. \tag{3.7}$$

A numerical calculation for GdIG yields, for example in a field H = 40 kOe, the following jumps of the angle θ: $\Delta\theta = 30°$ on CC′ and DD′, $\Delta\theta = 55°$ on AA′ and BB′, and $\Delta\theta = 10°$ on FF′ and GG′. On FF′ and GG′ the results also included a jumpwise change of the angle φ_0: $\{\varphi_0 = \pi/2,\ 7\pi/6,\ 11\pi/6\} \rightleftarrows \{\pi/6,\ 5\pi/6,\ 3\pi/2\}$. The width of the metastability region is $\Delta T \approx 0.2°K$ between the curves DD′ and BB′ and between AA′ and CC′, and $\Delta T \approx 0.3°K$ between the curves FF′ and GG′ (all in a field H = 40 kOe).

At H = 0 all eight states corresponding to the orientations of M_S (or M_{Fe}) along the easy axes of a cubic RIG are stable. If, for example we apply at $T = T_1$ (Fig. 4) a magnetic field along [111], then as the field is increased the transition to the collinear phase $\{\theta = 0\}$ occurs differently for different initial orientations of M. At the point P, the angle phases with $\varphi_0 = \pi/2$, $7\pi/6$, and $11\pi/6$ become unstable, and at the point Q at $\theta_0 = 90°$ the phases with $\varphi_0 = \pi/6$, $5\pi/6$, and $3\pi/2$ become unstable. The state with M ∥ [111] is stable up to the point R. All the foregoing is valid for a single-domain crystal. In real crystals, a domain structure occurs in region IV because of the influence of the demagnetizing fields. Then the stability-loss lines determine the boundaries of the existence of domains with corresponding directions of the magnetic moments.

All the curves in the diagrams were obtained by numerical calculation for GdIG. As a rule, the temperature dependence of the field on these curves, which is explicitly specified by equations of the type (3.5), (3.6), etc., cannot be obtained analytically. However, for the boundaries of the regions of stability of the collinear phases (Eqs. (2.11)) and also for the equal-angle curves θ = const, we can obtain an explicit T = T(H) dependence. To this end it is necessary to change over from the Brillouin function $B_S(x)$, which enters in χ_θ, to the reciprocal function $B_S^{-1}(x)$. For example, simple transformations of Eqs. (2.11) yield

$$\frac{1}{T_1} = \frac{kB_S^{-1}[(1 \pm 2K/MH)(\lambda M - H)/\lambda M_{R0}]}{\mu_R(\lambda M - H)}, \qquad \frac{1}{T_2} = \frac{kB_S^{-1}[(1 \mp 2K/MH)(\lambda M + H)/\lambda M_{R0}]}{\mu_R(\lambda M + H)}. \tag{3.8}$$

To conclude this section, we present numerical values of H*, H_1, H_2, and ΔT_{min} on the phase diagrams. For GdIG, assuming $H_2^{exch} = 250$ kOe near T_c and $K = 6.7 \times 10^3$ erg/cm^3[12], we obtain H* = 23 kOe and $\Delta T_{min} = 3°$. In a uniaxial crystal (H_2^{exch}, K, T_c for GdIG) we have H* = 28 kOe, $H_1 - H^* = H^* - H_2 = 400$ Oe, and $\Delta T_{min} = 3.5°$. Numerical estimates for other RIG yield H* ≈ 25 kOe and $\Delta T_{min} \approx 3°$ for TbIG, H* ≈ 50 kOe and $\Delta T_{min} \approx 60°$ for DyIG and H* ≈ 45 kOe and $\Delta T_{min} \approx 10°$ for HoIG.

4. DISCUSSION OF RESULTS

The anomalous behavior of the physical quantities at temperatures close to the compensation temperature is determined by the character of the phase diagrams. Many thermodynamic and kinetic quantities have singularities near the magnetic phase-transition points. Thus, in the second-order phase transition from a collinear phase to an angle phase there should be observed a jump in the specific heat ($\Delta C/C \sim 10°$), in Young's modulus, and in the magnetocaloric effect. Singularities of the thermodynamic quantities in weak fields are due to the fact that these quantities have different values at the phases $\{\theta = 0\}$ and $\{\theta = \pi\}$[13]. It can be shown that when the second-order phase-transition lines or the phase-stability boundaries are approached, the frequency of the ferrimagnetic resonance and the velocity of the domain wall tend to zero, the time required to reverse the magnetization of the sample is increased, the fluctuations of the magnetization increase sharply, etc.

In[14] they observed two peaks in the intensity of the light scattering when the temperature was varied near T_c in strong magnetic fields. These two peaks correspond to two phase-transition points on going through the angle phase. One can expect interesting singularities, characteristic of second-order phase transitions, in Raman light scattering (with change of frequency). The change of frequency $\Delta\omega$ of the scattered light approaches zero when the transition point is approached.

The most direct way of obtaining information concerning the phase diagram of RIG is to study the Faraday effect (FE). In RIG, the rotation of the plane of polarization of linearly polarized light in the visible region of the spectrum is due principally to the intense dipole transitions in the Fe^{3+} ions of the octahedral sublattice. In this case the magnitude and the sign of the FE are determined completely by the projection of the magnetization of the iron sublattice on the direction of light propagation. It is therefore easy to obtain the temperature and field dependences of the per-unit rotation α_F near T_c. Typical plots of $\alpha_F = \alpha_F(T)$ at H = const, for different orientations of the magnetic field, are shown

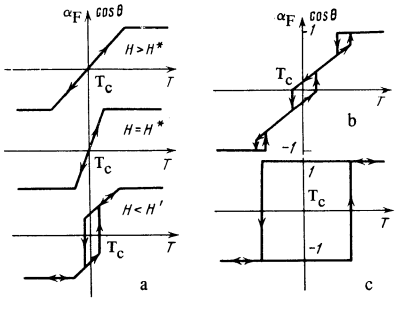

FIG. 5. Temperature dependence of cos θ and α_F near T_c for a cubic RIG: a) H ∥ [100], b) H ∥ [111] (strong fields), c) H ∥ [111] (weak fields).

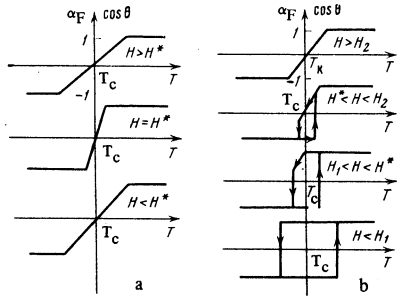

FIG. 6. Temperature dependence of cos θ and of the per unit rotation of the polarization plane α_F = const cos θ near T_c: a) **H** ⊥EA, b) **H**|| EA (uniaxial ferrimagnet).

in Figs. 5 and 6 (the light propagates along **H**). In weak fields, for all cases with the exception of **H** ⊥ EA of a uniaxial crystal, a temperature hysteresis of the FE should be observed. In strong fields, hysteresis loops arise only in single crystals with cubic anisotropy at **H** || [111]. Analogous phenomena should be observed if the FE is determined by the gyrotropy of the magnetic-susceptibility tensor (frequency-independent FE in the IR band, FE in the microwave region). The FE near T_c was investigated experimentally in[9,15]. A temperature hysteresis of the per-unit rotation of the polarization plane α_F was observed in weak fields and it was shown that the character of the temperature dependence of the FE varies with the field and with the character of the phase diagram when the type of anisotropy is changed. The experimental data are in good agreement with our calculations.

A very effective procedure is measurement of the thermodynamic quantities that experience abrupt changes on the phase boundaries, such as the magnetostriction[16,17] and the magnetocaloric effect[18]. Thermal effects in YbIG were investigated in[19,20]. Alben[21] investigated theoretically the phase diagram of this RIG. He did not, however, consider the metastable states and did not fully investigate the phase diagram in weak fields $H < \lambda M$; yet these questions are of prime significance when it comes to comparison with the existing experimental data.

As shown above, the ordering parameters in the angle phases are the angles between the magnetic sublattices and the crystallographic axes. In this sense, the phase transitions in question are of the "orientation" type, in which the orientation of the magnetic moments in the crystals changes (the Morin transition, transitions in uniaxial ferromagnets[22] or transitions connected with reorientation of the easy axis[23]).

It is of interest to trace the change of the symmetry in such a transition. In all the cases considered by us, the transition into the angle phase is accompanied by violation of the symmetry, in that the crystal is no longer invariant to rotation about a definite axis. Thus, in the cases corresponding to the phase diagrams shown in Figs. 1–4, the violated symmetry elements are rotations by 180° around the magnetic field, by an arbitrary angle around the EA, by multiples of $\pi/2$ around the [100] axis, and by multiples of $2\pi/3$ around [111]. We have also noted that a unique "degeneracy" with respect to energy exists in the angle phase, i.e., minimization yields several possible states that are equivalent energywise. It is easy to see that the "violated" symmetry elements transform these degenerate states into one another. It is interesting that the degeneracy makes it possible for a domain structure to exist in the flipping region also in strong fields.

We have used in the present paper the molecular-field approximation, which is equivalent to neglecting the magnetization fluctuations. However, the fluctuations of M increase sharply near second-order phase-transition points. It is therefore important to know the temperature interval $\Delta T = |T - T_{tr}|$ outside of which our results are valid. To consider this question, it is necessary to take into account the contribution of the energy of the magnetic inhomogeneities to the thermodynamic potential

$$\Delta E = \delta M^{-2}\{(\nabla M_x)^2 + (\nabla M_y)^2 + (\nabla M_z)^2\} \qquad (4.1)$$

(δ is the constant of exchange interaction between the iron sublattices).

If we use the criterion $\langle \Delta\eta^2 \rangle \ll \eta_0^2$ ($\langle \Delta\eta^2 \rangle$ is the fluctuation and η_0 the equilibrium value of the ordering parameter) then, as shown by Ginzburg[24], the temperature interval ΔT can be estimated from the formula

$$\Delta T / T_{tr} = k^2 T_{tr}\, b^2 / a_T' \delta^3 \equiv \xi, \qquad (4.2)$$

where k is Boltzmann's constant, a and b are the coefficients of expansion (3.1), and δ is obtained from (4.1). In our case $\xi = (0.1-1)\,(H/H_1^{exch})^3$. In a field $H = 2 \times 10^4$ Oe, this yields $\xi \sim 10^{-6}-10^{-7}$, i.e., the transition is very "abrupt." For a comparison, we indicate that $\xi \approx 10^{-1}$ for the phase transition at the Curie point. The physical reason for the suppression of the fluctuations is the considerable increase of the correlation radius r for the investigated transitions. Whereas near the Curie point we have $r_c \sim a[(T - T_c)/T_c]^{-1/2}$ (a is the lattice constant), in our case $r \sim (H_1^{exch}/H)^{1/2} r_c$. From the point of view of the applicability of Landau's theory, the "orientation" transitions are intermediate between the transitions in superconductors ($\xi \sim 10^{-16}$) and the ferroelectric phase transitions ($\xi \sim 10^{-3}$).

APPENDIX

We reduce the thermodynamic potential (2.5) to the form (2.6).

Uniaxial anisotropy. Since $W_R \approx \lambda M^2$, we can assume, accurate to terms of order $W_R/\lambda M^2$, that $\mathbf{M}_R \parallel \mathbf{H}_{eff}$, and consequently

$$W_a = K_{Fe}\frac{(\mathbf{Mn})^2}{M^2} + K_R(H_{eff})\frac{(\mathbf{H}_{eff}\mathbf{n})^2}{H_{eff}^2}, \qquad (A.1)$$

where **n** is a unit vector in the EA direction. Since we are considering a small temperature region near T_c, we can disregard the temperature dependence of the anisotropy constants. Expanding $(\mathbf{H}_{eff} \cdot \mathbf{n})^2/H_{eff}^2$ and $K_R(H_{eff})$ in powers of $H/\lambda M$, we obtain

$$W_a = K\frac{(\mathbf{Mn})^2}{M^2} + K_R^0\frac{H}{\lambda M} g(\theta)\cos\theta, \qquad (A.2)$$

where $g(\theta) = (\beta + 2)\cos^2\theta - 2$ for **H** || **n** and $g(\theta) = (\beta = 2)\sin^2\theta$ for **H** ⊥ **n**; $\beta = (\partial K_R/\partial H_{eff})\lambda M/K_R^0 \sim 1$; $K_R^0 = K_R(\lambda M)$; $K \approx K_{Fe} + K_R^0$ is the effective anisotropy constant. After substituting (A.2) in (2.5) we obtain

$$\Phi = -MH\cos\theta\left(1+\frac{K_R^0}{\lambda M^2}g(\theta)\right) - \int_0^{H_{\text{eff}}} M_R\, dH_{\text{eff}} + Kf(\theta,\varphi) \quad \text{(A.3)}$$

which coincides with (2.6) apart from terms $\sim K_R^0/\lambda M^2$.

Cubic anisotropy. At $W_R \ll \lambda M^2$ the anisotropy energy is given by

$$W_a = K_{\text{Fe}} \sum_{i<j}^{3} \frac{(\mathbf{M}\mathbf{n}_i)^2(\mathbf{M}\mathbf{n}_j)^2}{M^4} + K_R(H_{\text{eff}}) \sum_{i<j}^{3} \frac{(\mathbf{H}_{\text{eff}}\mathbf{n}_i)^2(\mathbf{H}_{\text{eff}}\mathbf{n}_j)^2}{H_{\text{eff}}^4}, \quad \text{(A.4)}$$

$\mathbf{n}_1$, $\mathbf{n}_2$, and $\mathbf{n}_3$ are unit vectors along the axes [100], [010], and [001], respectively. In the first approximation with respect to $H/\lambda M$, we have at $\mathbf{H} \parallel [100]$

$$W_a = (K_{\text{Fe}} + K_R^0)\sum_{i<j}^{3} \alpha_i\alpha_j + K_R^0 \frac{H}{\lambda M} g(\alpha_1,\alpha_2,\alpha_3)\cos\theta, \quad \text{(A.5)}$$

$$\Phi = -MH\cos\theta\left(1+\frac{K_R^0}{\lambda M}g(\alpha_1,\alpha_2,\alpha_3)\right) - \int_0^{H_{\text{eff}}} M_R\, dH_{\text{eff}} + K\sum_{i<j}^{3}\alpha_i\alpha_j. \quad \text{(A.6)}$$

Here α_1, α_2, and α_3 are the direction cosines of the magnetization $\mathbf{M}$, and

$$g(\alpha_1,\alpha_2,\alpha_3) = (4+\beta)\sum_{i<j}^{3}\alpha_i\alpha_j + \alpha_1^2 + \alpha_2^2.$$

Just as in the uniaxial case, (A.6) coincides with (2.6) apart from terms of order $K_R^0/\lambda M^2$.

If $\mathbf{H} \parallel [111]$, then

$$W_a = K\sum_{i<j}^{3}\alpha_i\alpha_j + K_R^0\frac{H}{\lambda M}\Big\{(4+\beta)\cos\theta\sum_{i<j}^{3}\alpha_i\alpha_j + \frac{1}{\sqrt{3}}[(\alpha_1^2+\alpha_2^2)\alpha_3 + (\alpha_1^2+\alpha_3^2)\alpha_2 + (\alpha_2^2+\alpha_3^2)\alpha_1]\Big\}. \quad \text{(A.7)}$$

The second term in (A.7) does not contain $\cos\theta$ as a factor, in contrast to the case $\mathbf{H} \parallel [100]$. Therefore at $\theta \approx \pi/2$ this term can become comparable with the term $-MH\cos\theta$ in the thermodynamic potential. This could lead to a change in the type of phase transition (second order → first order), were the minimization of the potential, with account taken of only the term $K\sum_{i<j}^{3}\alpha_i\alpha_j$, to lead to a second-order phase transition from the collinear phases to the angle phase. However, at $\mathbf{H} \parallel [111]$ this transition is already of first order even without allowance for the second term in (A.7). The term proportional to $H/\lambda M$ in (A.7) thus does not lead to new effects and can be disregarded because of its smallness.

In conclusion, we note that it is easy to consider in similar fashion also the terms describing anisotropic interactions between sublattices, such as anisotropic exchange.

[1] S. V. Tyablikov, Metody kvantovoĭ teorii magnetizma (Methods of the Quantum Theory of Magnetism), Nauka, 1965.

[2] A. A. Gusev, Kristallografiya **4**, 695 (1959) [Sov. Phys. Crystallogr. **4**, 655 (1959)].

[3] A. Clark and E. Callen, J. Appl. Phys. **39**, 5972 (1968).

[4] B. P. Goranskiĭ and A. K. Zvezdin, Zh. Eksp. Teor. Fiz., Pis'ma Red. **10**, 196 (1969) [JETP Lett. **10**, 124 (1969)].

[5] A. S. Pakhomov and V. A. Gerbutov, Fiz. Tverd. Tela **13**, 10 (1971) [Sov. Phys. Solid State **13**, 7 (1971)].

[6] J. H. Van Vleck, Electric and Magnetic Susceptibilities. Oxf. Univ. Press., New York, 1932.

[7] K. A. Wickersheim, Phys. Rev. **122**, 1376 (1961).

[8] S. Geschwind, Phys. Rev. **121**, 363 (1961).

[9] G. D. Mee, Contemp. Phys. **8**, 385 (1967).

[10] A. H. Bobeck, E. G. Spencer, L. G. Van Uitert, S. C. Abrahams, R. L. Barns, W. H. Grodkiewicz, R. C. Sherwood, P. H. Schmidt, D. H. Smith, and E. M. Walters, Appl. Phys. Lett. **17**, 131 (1970).

[11] L. D. Landau and E. M. Lifshitz, Statisticheskaya fizika (Statistical Physics), Nauka, 1964.

[12] K. P. Belov, M. A. Belyanchikova, R. Z. Levitin, and S. A. Nikitin, Redkozemel'nye ferro- i antiferromagnetiki (Rare-Earth Ferro- and Antiferromagnetics), Nauka, 1965.

[13] K. P. Belov and S. A. Nikitin, Zh. Eksp. Teor. Fiz. **58**, 937 (1970) [Sov. Phys. JETP **31**, 505 (1970)].

[14] R. V. Pisarev, I. G. Siniĭ, and G. A. Smolenskiĭ, Zh. Eksp. Teor. Fiz. **57**, 737 (1969) [Sov. Phys. JETP **30**, 404 (1970)].

[15] E. A. Smirnova, V. I. Smirnov, Yu. I. Ukhanov, and V. A. Petrusevich, Zh. Eksp. Teor. Fiz., Pis'ma Red. **11**, 435 (1970) [JETP Lett. **11**, 293 (1970)].

[16] K. P. Belov, R. Z. Levitin, B. K. Ponomarev, and Yu. F. Popov, Zh. Eksp. Teor. Fiz., Pis'ma Red. **10**, 13 (1969) [JETP Lett. **10**, 8 (1969)].

[17] R. Z. Levitin, B. K. Ponomarev, and Yu. F. Popov, Zh. Eksp. Teor. Fiz. **59**, 1952 (1970) [Sov. Phys. JETP **32**, 1056 (1971)].

[18] K. P. Belov, L. A. Chernikova, E. V. Talalaeva, R. Z. Levitin, T. V. Kudryavtseva, S. Amadezi, and V. I. Ivanovskiĭ, Zh. Eksp. Teor. Fiz. **58**, 1923 (1970) [Sov. Phys. JETP **31**, 1035 (1970)].

[19] R. Buchmann and A. Clark, Solid State Commun. **7**, 1087 (1969).

[20] A. Clark and R. Alben, J. Appl. Phys. **41**, 1195 (1970).

[21] R. Alben, Phys. Rev. B **2**, 2767 (1970).

[22] H. Thomas, Phys. Rev. **187**, 630 (1969).

[23] H. Horner and C. M. Varma, Phys. Rev. Lett. **20**, 845 (1968).

[24] V. L. Ginzburg, Fiz. Tverd. Tela **2**, 2031 (1960) [Sov. Phys. Solid State **2**, 1824 (1961)].

Translated by J. G. Adashko
35